Noise analysis of aircraft departure procedures using MONTE CARLO simulation

Smits, Tommy; Hartjes, Sander; Mitici, Mihaela

Publication date
2018

Document Version
Accepted author manuscript

Published in
Proceedings of the Winter Simulation Conference

NOISE ANALYSIS OF AIRCRAFT DEPARTURE PROCEDURES USING MONTE CARLO SIMULATION

Tommy Smits
Sander Hartjes
Mihaela Mitici

Air Transport & Operations, Delft University of Technology
Kluyverweg 1
Delft, 2600 GB, THE NETHERLANDS

ABSTRACT

During arrival and departure procedures at an airport, aircraft generate noise. High levels of noise during these terminal procedures can have a negative impact on the communities located near the airport. We assess the impact of the noise generated by a standard instrument departure of a twin-engine narrow body mid-range aircraft over the communities nearby Amsterdam Airport Schiphol, the Netherlands. During the departure procedure, we consider a stochastic flight trajectory that is subject to lateral position errors. We estimate, using Monte Carlo simulation, the distribution of the sound exposure level and of the number of awakenings generated by a departure. We also identify the residential areas where the number of awakenings are overestimated or underestimated, when comparing a stochastic and a deterministic departure approach. Lastly, we approximate the distribution of the noise level for a generic aircraft departure, which can be further employed for further optimization of departure procedures.

1 INTRODUCTION

The noise generated by aircraft during an arrival/departure at an airport is of continuous concern for the people living in the vicinity of an airport. High levels of noise during a flyover can generate annoyance and even awake people during nighttime.

To reduce the negative impact of the aircraft noise on the communities nearby large airports, over the years, several noise abatement measurements have been adopted. One frequently employed measure is to enforce a maximum yearly number of flight operations, as well as a day-evening-night maximum noise level allowed around the airport. Moreover, for a single flight, the International Civil Aviation Organisation (ICAO) de-

fined two noise abatement departure procedures such that the total area impacted by the noise is limited [8]. Several improvements of the noise abatement terminal procedures have been proposed in the last years. [6, 7, 14] have developed a tool that optimizes aircraft arrival and/or departures with respect to fuel consumptions and number of awakenings. Similar techniques have been developed in [16]. [10, 11] have developed a lexicographic optimization technique to deal with aircraft departure trajectories such that noise annoyance is minimized. [3,15] have proposed a dynamic programming technique for minimizing noise in runway-independent aircraft operations.

In the trajectory optimization techniques above, however, the inherent uncertainty of a flight trajectory, such as, for instance, aircraft position errors, the impact of wind and other atmospheric estimation errors on the nominal trajectory, are not taken into account. In [12] a 4D trajectory optimization is performed to minimize fuel consumption, flight time, operative cost, noise impact and persistent contrail formation. Following optimization, the reference trajectory is subject to stochastic parameters such as position error, velocity error, mass errors. The impact of system uncertainties is evaluated by means of Monte Carlo simulation. [4] estimates the noise load of a helicopter by means of a Monte Carlo simulation. An analysis of the sound exposure level around JFK airport is conducted in [1] by means of a Monte Carlo simulation. A noise contour plot of the mean sound exposure level around JFK airport for one day of operations is determined.

In this paper we assess the impact of stochastic aircraft position error on the distribution of the sound noise exposure and the expected number of awakenings generated by a single aircraft departure. We make use of a Geographic information system (GIS) of the population density for residential areas located in the vicinity of Amsterdam Airport Schiphol (AMS) and of a noise computation methodology introduced by the Federal Aviation Administration. A Monte Carlo simulation of a standard instrument departure (Spijkerboor) from AMS, the Netherlands, is conducted. The simulation results are compared against a nominal departure procedure, where the influence of system uncertainties is not considered. We show that, in comparison to the simulation approach, the deterministic approach overestimates the number of awakenings in the residential areas nearby the nominal trajectory and underestimates the number of awakenings in the areas further away from the nominal trajectory. We also approximate the distribution of the sound exposure level for a twin-engine narrow body mid-range aircraft departure, which can be further used to speed-up noise optimization methods, while taking into account system uncertainties.

This paper is organized as follows. In Section 2 we define an aircraft point-mass model that takes into account aircraft lateral measurement errors, the sound exposure level model, following the INM methodology, and the awakenings model. In Section 3 we outline the results of simulating a flight departure subject to lateral measurement errors and the impact on awakening. We consider a standard instrument departure from AMS: the Spijkerboor departure. Lastly, we determine an approximation of the distribution of the sound level exposure as a function of the model parameters. In Section 4 we summarize the results and provide conclusions.

2 MODEL DESCRIPTION

In this section we first introduce an aircraft point-mass model, which takes into account lateral measurement errors. We next define a methodology to estimate the level of sound exposure that people living in the vicinity of an airport experience during an aircraft departure from AMS. Based on the sound exposure level, the percentage of awakenings in a residential area, i.e., the percentage of people that is expected to awake due to a single flyover, is determined.

2.1 Aircraft model

We define a stochastic point-mass model to represent an aircraft during terminal operations that is subject to lateral error measurement. Let x_i, y_i, h_i denote the latitude, longitude and altitude of the aircraft at waypoint i on the nominal aircraft trajectory, respectively. Let ε_i denote the measurement error in the lateral position at waypoint i.

Let $V_{i,TAS}$ and W_i denote the true aircraft speed and aircraft weight, at waypoint i, respectively; g_0 is the gravitational acceleration, $T_i, D_i, \dot{m}_{f,i}, \chi_i, \mu_i$ are the thrust, drag, fuel mass flow, heading angle and bank angle at waypoint i, respectively.

We further make the following assumptions: i) the Earth is flat and non-rotating; ii) the flight is coordinated; iii) the flight path angle is considered sufficiently small ($\gamma < 15^\circ$).

Additionally, it is assumed that there is an equilibrium present for the forces normal to the flight path. Given these assumptions, the equations of motions are represented by a set of difference equations as follows:

$$x_{i+1} = x_i + \Delta \sin\chi_i + \varepsilon_{i+1}\sin\chi_i \tag{1}$$

$$y_{i+1} = y_i + \Delta \cos\chi_i + \varepsilon_{i+1}\cos\chi_i \tag{2}$$

$$h_{i+1} = h_i + \Delta \tan\gamma_i \tag{3}$$

$$W_{i+1} = W_i + \Delta \dot{m}_{f,i} g_0 \frac{1}{V_i \sin\gamma_i} \tag{4}$$

$$V_{i+1,TAS} = V_{i,TAS} + \Delta g_0 \left[\frac{T_i - D_i}{W_i} - \sin\gamma_i\right] \frac{1}{V_{i,TAS}\sin\gamma_i} \tag{5}$$

$$\chi_{i+1} = \chi_i + \frac{g_0 \tan(\mu_i)}{V_{i,TAS}^2 \sin\gamma_i}, \text{where} \tag{6}$$

$$\varepsilon_{k_{j+1}} = \alpha\varepsilon_{k_j} + (1-\alpha)\varphi, j \in \{0,1,2,\ldots,n\}, k_1 < k_2 < k_3 < \ldots < k_n, k_j \in \mathbb{N} \tag{7}$$

$$\varepsilon_{i+1} = \varepsilon_i + \frac{\varepsilon_{k_{j+1}} - \varepsilon_{k_j}}{k_{j+1} - k_j}, i \in [k_j, k_{j+1}), i \in \mathbb{N} \tag{8}$$

with $\alpha \in (0,1), \varphi \sim N(0, \sigma_\varphi^2), \varepsilon_{k_0} = 0$, Δ the distance flown between 2 consecutive waypoints.

We further ensure that $\varepsilon_{k_j} \sim N(0, \sigma_{RNP}^2), \forall j \in \{0,1,2,\ldots,n\}$, where $\sigma_{RNP} = 926$m [9]. The value $\sigma_{RNP} = 926$m is based on the required navigation performance (RNP1)

specified in the Performance Based Navigation report of Amsterdam Schiphol Airport [9], where an RNP of 1NM (Nautical Mile) is required during the arrival and departure phase of a flight. The RNP systems provide on-board navigation capabilities such that the aircraft deviations from a desired flight track, given nominal environmental conditions, are bounded. Thus, an RNP-compliant navigation restricts the distribution of the navigation system error.

Now, given $\varepsilon_{k_j} \sim N(0, \sigma^2_{RNP})$, for a fixed $\alpha \in (0,1)$,

$$\sigma^2_{\varphi} = \sigma^2_{RNP} \frac{1-\alpha^2}{(1-\alpha)^2}.$$

Lastly, for low altitudes and airspeeds, the equivalent airspeed, denoted by V_{EAS}, is used as an approximation for the indicated airspeed, as follows:

$$V_{EAS} = V_{TAS}\sqrt{\rho/\rho_0}. \tag{9}$$

Using equation (9), the difference equations (5) - (6) become:

$$V_{i+1,EAS} = V_{i,EAS}\sqrt{\rho_0/\rho} + \Delta g_0 \left[\frac{T_i - D_i}{W_i} - \sin\gamma_i\right]\sqrt{\rho_0/\rho} + \frac{1}{2\rho}\frac{\partial\rho}{\partial h_i}\Delta^2 V^2_{EAS,i}\sin\gamma_i\sqrt{\rho_0/\rho} \tag{10}$$

$$\chi_{i+1} = \chi_i + \frac{g_0\tan(\mu_i)}{V_{i,EAS}\sqrt{\rho_0/\rho}}, \tag{11}$$

where $\frac{\partial\rho}{\partial h_i}$ is the derivative of the ambient air density with respect to the altitude.

2.2 Sound exposure level model

To determine the sound level exposure *SEL* (db) at a given location, i.e., the aircraft flyover noise at a location, we implement the INM methodology [5]. INM is the standard methodology for noise impact assessment of the Federal Aviation Administration since 1978.

Firstly, we define a grid of points over residential areas in the vicinity of an airport. We refer to these grid points as observer locations. For the numerical analysis, we have defined a rectangular of dimension 80×80 km around AMS, the Netherlands, with a relatively coarse mesh (0.5×0.5 km). Next, following the model in Section 2.1 and the INM methodology, the flight path is described as a sequence of segments. Figure 1 shows an example of a segment-based flight path and a set of observer locations. Lastly, the distance between the flight segment and a given observer point is determined. Figure 2 shows the geometry of the flight segment relative to an observer point.

We determine outdoor *SEL* at a specific observer location by selecting appropriate sound levels using a noise-thrust-distance (NTD) look-up table corresponding to the

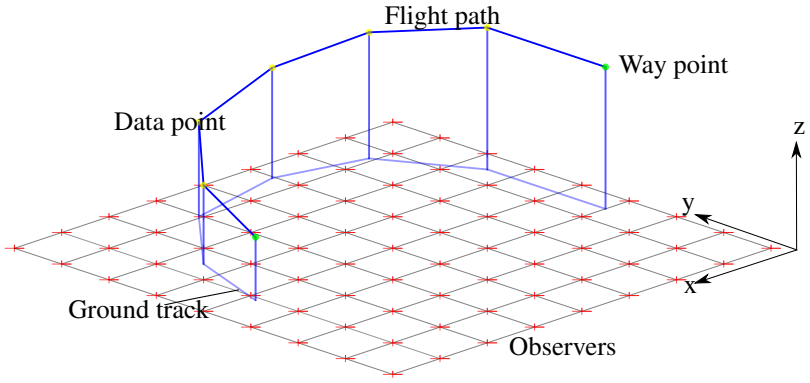

Figure 1: Grid of points (observer locations) in the vicinity of an airport.

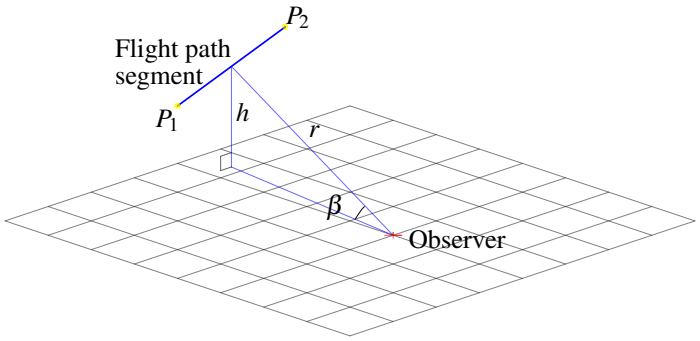

Figure 2: Geometry of the flight segment and a specific observer point, where h is the flight altitude, r is the minimum distance between the location of the observer and the flight segment.

distance between the aircraft and the observer point. The NTD table is defined by the INM methodology and contains the noise exposure levels for specific reference conditions. The uncorrected NTD noise-level values, which are derived from the NTD table, are further adjusted by a fractional component, which depends on the geometry of the flight segment relative to the observer point, as well as other prevailing operational conditions such as speed adjustment and lateral attenuation adjustment [13]. Lastly, indoor *SEL* is determined by subtracting an amount of 15 dB from the outdoor *SEL*, where 15 dB represents the average transmission loss for a house. We consider only indoor *SEL* that are larger or equal to 50 dB. Sound levels below 60 dB are ignored since they do not generate awakenings [13]. Moreover, for computational efficiency, we compute *SEL* only at observer locations that are populated.

2.3 Awakenings model

Given the level of indoor *SEL* computed according to the methodology in Section 2.2, the American National Standards Institute (ANSI) defines the percentage of awakenings *PA*, i.e., the percentage of people that are likely to be awakened from sleep when they are at home, as follows [2],

$$PA = \frac{1}{1+e^{-(-6.8884+0.04444SEL_{indoor})}}. \tag{12}$$

Further, knowing the density of the population in the residential areas around an airport, the absolute number of people that are awakened (*NA*) is determined. In this paper we consider a geographic information system (GIS) based on the population density in the vicinity of AMS. This data is used to define population densities at the grid observer points.

3 MONTE CARLO SIMULATION OF AIRCRAFT DEPARTURE

In this section we outline the results of the Monte Carlo simulation of a standard instrument departure from AMS (Spijkerboor departure). For the numerical analysis, we consider one aircraft performance model corresponding to a twin-engine narrow body mid-range aircraft with two engines and an initial weight of 68,000 kg.

3.1 Spijkerboor departure

Spijkerboor flight departure is located in the vicinity of the cities Haarlem (159,300 inhabitants), Hoofddorp (75,600 inhabitants) and Amsterdam (853,312 inhabitants), see Figure 3. The trajectory starts at a screen height of 50 ft with the landing gear retracted and departure flaps selected. Full take-off thrust will be used until at least 1500 ft altitude, while maintaining its initial velocity. Beyond that altitude, the thrust is set back to maximum climb settings and the aircraft is also allowed to turn. When reaching 3000 ft altitude, the aircraft accelerates to the airspeed where the flaps and slats are fully retracted. The terminal conditions for this departure are an airspeed of 250 kts and an altitude of 6000 ft. During the entire departure, the aircraft is not allowed to decelerate or decent. To ensure RNP-compliance, the aircraft is assumed to be equipped with RNP navigation system, which contains an FMS with GPS sensors.

We have developed a Monte Carlo simulation of Spijkerboor departure using equations (1) - (11), Section 2.1. The simulation takes as input the states of the aircraft (latitude, longitude, altitude, velocity, weight, heading angle) and the stochastic lateral measurement error. We have divided the nominal trajectory in segments, in accordance with the INM methodology (see Section 2.2). Each segment is delimited by two consecutive waypoints. The lateral measurement errors are correlated across these waypoints (see equations (7)- (8)), using exponential smoothing with smoothing factor $\alpha = 0.3$.

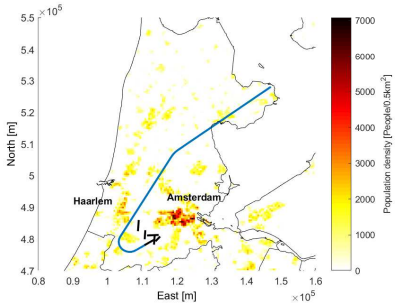

Figure 3: The Spijkerboor standard instrument departure with the population density.

Figure 4 shows the expected level of sound exposure and the number of awakenings generated by a flyover. The results are shown only for the populated areas. In comparison with a deterministic aircraft model for a nominal trajectory, where the uncertainty in the aircraft position is not considered, the number of awakenings are overestimated in the residential areas close to the nominal trajectory and underestimated in the residential areas farther away from the trajectory (see Figure 5a). Moreover, the number of awakenings in the residential areas outside of the trajectory turn is underestimated when a deterministic model is employed (see Figure 5b).

Figure 6 identifies the residential areas where the sound exposure level is underestimated or overestimated when a deterministic approach is used. These results are also supported by the standard deviation of the level of sound exposure (see Figure 7) which shows a larger spread outside of the turn.

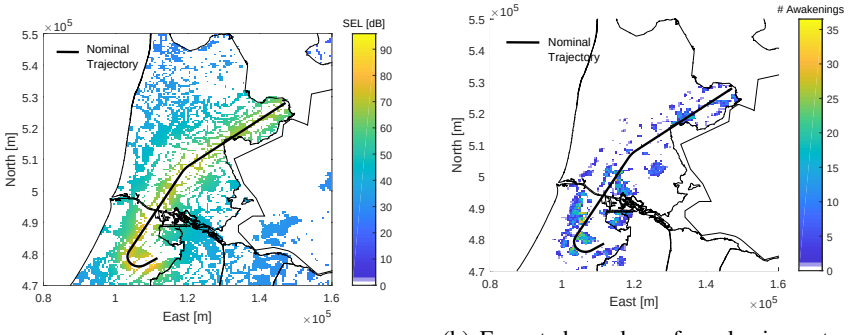

(a) $\mathbb{E}[SEL]$ at each populated grid point

(b) Expected number of awakenings at each populated grid point.

Figure 4: Monte Carlo simulation of Spijkerboor departure.

3.2 Approximating the distribution of the sound level exposure

In this section we estimate the distribution of the sound level exposure as a function of the model parameters. We consider a general grid of 1km $\times$ 80 km with a mesh of

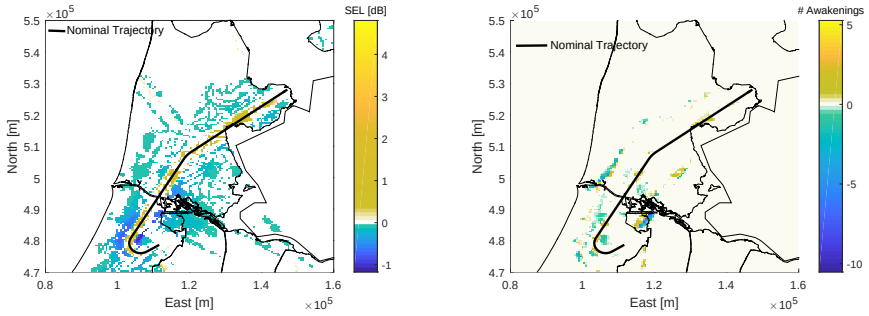

(a) $SEL_i^{Nominal} - \mathbb{E}[SEL]_i^{MonteCarlo}$ at grid point i.

(b) $NA_i^{Nominal} - \mathbb{E}[NA]_i^{MonteCarlo}$ at grid point i.

Figure 5: Difference between SEL and the number of awakenings (NA) generated using a deterministic, nominal trajectory and Monte Carlo simulation for a grid point - Spijkerboor departure from AMS. There is a total of 8193 awakenings generated by the deterministic, nominal trajectory, whereas there is a total of 8297 expected awakenings generated in the stochastic approach.

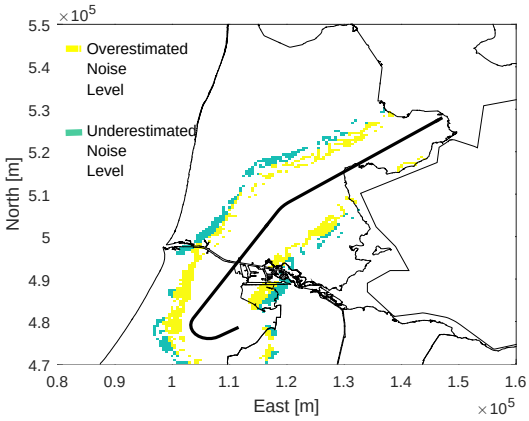

Figure 6: Difference between SEL determined using a deterministic, nominal trajectory and Monte Carlo simulation. The yellow grid points indicate areas where SEL is overestimated by the deterministic approach. The green grid points indicate areas where SEL is underestimated by the deterministic approach.

0.5×0.5 km. We consider a generic flight segment, in steady state, at varying altitudes (h) over the grid and at varying minimum distance r from the segment. We consider a lateral position error $\varepsilon \sim N(0, \sigma_{RNP}^2)$ over the flight segment. Using Monte Carlo simulation we estimate σ_{SEL} as a function of the flight altitude h and minimum distance between the segment and an observer point (see Table 1). We corrected the estimation of σ_{SEL} with the turn radius at varying altitudes. We also correct for the observer location being inside or outside the turn (see also Section 4). For computational speed-

ups of, for instance, a trajectory optimization of a twin-engine narrow body mid-range aircraft with the RNP requirements specified in [9], the estimated distribution of SEL can be readily employed. In turn, with this approach we can readily determine the number of awakenings generated by a a twin-engine narrow body mid-range aircraft flying over a generic area.

4 CONCLUSIONS

An assessment of the noise distribution and number of awakenings generated by the departure from AMS of a twin-engine narrow body mid-range aircraft has been conducted by means of a Monte Carlo simulation, together with a standard INM methodology for noise impact assessment specified by the Federal Aviation Administration. A case study for the Spijkerboor departure from AMS has been conducted. The simulations results have been compared with a deterministic, nominal departure procedure. Residential areas in the vicinity of AMS have been identified where the deterministic approach has underestimated or overestimated the number of awakenings. The distribution of the sound exposure level for a twin-engine narrow body mid-range aircraft departure was also determined, which can be further used to speed-up noise optimization methods, while taking into account system uncertainties. Future research plans include investigating the impact of the stochasticity of several other states of the aircraft such as aircraft weight and altitude on the sound exposure levels.

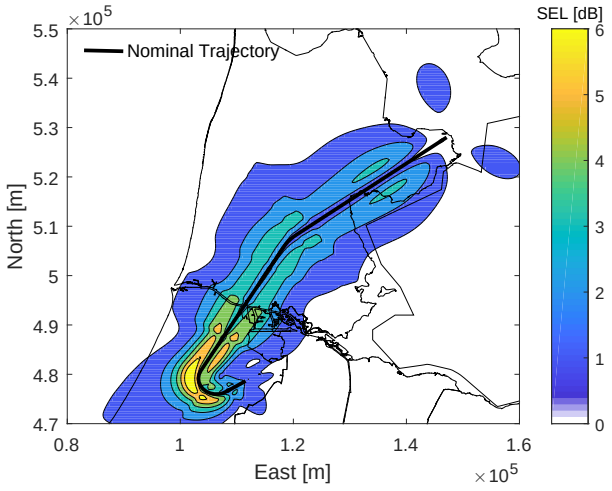

Figure 7: Contour of σ_{SEL} for Spijkerboor departure.

Table 1: σ_{SEL} (dB) as a function of the flight altitude h (ft) and the distance between a flight segment and a specific observer location r (m).

	1000 ft	1500 ft	2000 ft	$h \quad \cdots \quad h$	5500 ft	6000 ft	6500 ft
0 m	8.041	6.913	6.108	$\cdots$	3.618	3.124	2.771
250 m	8.039	6.911	6.107	$\cdots$	3.616	3.124	2.770
500 m	8.038	6.909	6.105	$\cdots$	3.615	3.121	2.769
750 m	8.036	6.907	6.104	$\cdots$	3.613	3.120	2.767
r $\vdots$ r	$\vdots$	$\vdots$	$\vdots$	$\cdots$ $\vdots \quad \ddots \quad \vdots$ $\cdots$	$\vdots$	$\vdots$	$\vdots$
39250 m	0.171	0.170	0.174	$\cdots$	0.180	0.184	0.189
39500 m	0.170	0.169	0.173		0.180	0.183	0.189
39750 m	0.168	0.169	0.171	$\cdots$	0.179	0.183	0.188
40000 m	0.167	0.168	0.170	$\cdots$	0.178	0.181	0.187

References

[1] Douglas Allaire, George Noel, Karen Willcox, and Rebecca Cointin. Uncertainty Quantification of an Aviation Environmental Toolsuite. *Reliability Engineering & System Safety*, 126:14–24, 2014.

[2] ANSI/ASA. Quantities and Procedures for Description and Measurement of Environmental Sound - Part 6: Methods for Estimation of Awakenings Associated with Outdoor Noise Events Heard in Homes. *Washington DC, USA*, 2008.

[3] Ella M Atkins and Min Xue. Noise-sensitive Final Approach Trajectory Optimization for Runway-Independent Aircraft. *Journal of Aerospace Computing, Information, and Communication*, 1(7):269–287, 2004.

[4] József Bera and László Pokorádi. Monte-Carlo Simulation of Helicopter Noise. *Acta Polytechnica Hungarica*, 12(2):21–32, 2015.

[5] E.R. Boeker and E. Dingens. Integrated Noise Model (INM) version 6.0 Technical Manual, FAA-AEE-02-01, U.S. Department of Transportation. Technical report, 2006.

[6] S Hartjes, J Dons, and HG Visser. Optimization of Area Navigation Arrival Routes for Cumulative Noise Exposure. *Journal of Aircraft*, 51(5):1432–1438, 2014.

[7] Vinh Ho-Huu, Sander Hartjes, Hendrikus G Visser, and Richard Curran. An Efficient Application of the MOEA/D Algorithm for Designing Noise Abatement Departure Trajectories. *Aerospace*, 4(4):54, 2017.

[8] ICAO. Procedures for Air Navigation Services Aircraft Operations (PANS-OPS) vol. i, Flight Procedures (4th ed.), International Civil Aviation Organisation (ICAO), Montreal, Canada (1993) doc. 8168-OPS/611. Technical report, 1993.

[9] PBN. Performance Based Navigation (PBN):ROADMAP for the Kingdom of the Netherlands 2010-2020, version 1.0, Ministry of Transport, Public Works and Water Management, the Netherlands. Technical report, 2010.

[10] Xavier Prats, Vicenç Puig, Joseba Quevedo, and Fatiha Nejjari. Lexicographic Optimisation for Optimal Departure Aircraft Trajectories. *Aerospace science and technology*, 14(1):26–37, 2010.

[11] Xavier Prats, Vicenç Puig, Joseba Quevedo, and Fatiha Nejjari. Multi-objective Optimisation for Aircraft Departure Trajectories Minimising Noise Annoyance. *Transportation Research Part C: Emerging Technologies*, 18(6):975–989, 2010.

[12] Subramanian Ramasamy, Roberto Sabatini, Alessandro G Gardi, and Yifang Liu. Novel Flight Management System for Real-time 4-dimensional Trajectory Based Operations. In *AIAA Guidance, Navigation, and Control (GNC) Conference*, page 4763, 2013.

[13] Hendrikus G Visser and RA Wijnen. Optimization of Noise Abatement Departure Trajectories. *Journal of Aircraft*, 38(4):620–627, 2001.

[14] Hendrikus G Visser and Roland AA Wijnen. Optimisation of Noise Abatement Arrival Trajectories. *The aeronautical journal*, 107(1076):607–615, 2003.

[15] Min Xue and Ella M Atkins. Noise-minimum Runway-Independent Aircraft Approach Design for Baltimore-Washington International Airport. *Journal of Aircraft*, 43(1):39–51, 2006.

[16] Katherine Feng Zou and John-Paul Clarke. Adaptive Real-time Optimization Algorithm for Noise Abatement Approach Procedures. In *AIAA's 3rd Annual Aviation Technology, Integration, and Operations (ATIO) Forum*, page 6771, 2003.